Magazine of Concrete Research
Volume 65 Issue 15

Effects of specimen size and shape on compressive and tensile strengths of self-compacting concrete with or without fibres
Aslani

Magazine of Concrete Research, 2013, **65**(15), 914–929
http://dx.doi.org/10.1680/macr.13.00016
Paper 1300016
Received 08/01/2013; revised 24/03/2013; accepted 27/03/2013
Published online ahead of print 07/06/2013

ICE Publishing: All rights reserved

ice
Institution of Civil Engineers
publishing

Effects of specimen size and shape on compressive and tensile strengths of self-compacting concrete with or without fibres

Farhad Aslani
Centre for Built Infrastructure Research, School of Civil and Environmental Engineering, University of Technology Sydney, Australia

Self-compacting concrete (SCC) can be placed and compacted under its own weight. Modifications in the mix design of SCC may significantly influence the material's mechanical properties. Therefore, it is vital to investigate whether all the assumed hypotheses about conventional concrete also hold true for SCC structures. This paper discusses an experimental programme that was carried out to study the effects of specimen size and shape on the compressive and tensile strength of SCC and fibre reinforced SCC. For this purpose, cube specimens with 100 and 150 mm dimensions and cylinder specimens with 100 × 200 and 150 × 300 mm dimensions were casted. The experimental programme examined four SCC mixtures: plain SCC, and steel-, polypropylene- and hybrid-fibre reinforced SCC. Compressive and tensile strengths were tested after 3, 7, 14, 28 and 56 days. The paper also investigates correlations between compressive and tensile strengths and the size and shape of the specimen.

Notation

B	empirical constant
d	diameter of cylinder specimen: cm
d_a	maximum aggregate size: mm
f'_c	N-SCC mix compressive strength: MPa
f'_{cDS}	DS-SCC mix compressive strength: MPa
f'_{cfD}	D-SCC mix compressive strength: MPa
$f'_{cmy}(d)$	compressive strength with size of general cylinder: MPa
f_{ct}	N-SCC mix tensile strength: MPa
f'_{cfS}	S-SCC mix compressive strength: MPa
$f'_{cmu}(d)$	compressive strength of cube: MPa
$f_{ctmy}(d)$	tensile strength of cylinder: MPa
f_{fctD}	D-SCC mix tensile strength: MPa
f_{fctDS}	DS-SCC mix tensile strength: MPa
f_{fctS}	S-SCC mix tensile strength: MPa
h	height of cylinder specimen: cm
l_0	width of crack band: mm
l_f/d_f	aspect ratio
R. I.	fibre reinforcing index
V_f	fibre volume fractions
α	empirical constant
λ_o	empirical constant
$\sigma_N(d)$	nominal strength: MPa

Introduction

In the last three decades, there have been significant improvements in concrete technology, and these improvements have led to the development of high-performing concrete, such as self-compacting concrete (SCC). SCC is a highly workable, non-segregating concrete that can easily reach remote corners, fill congested formworks and provide reinforcement without any vibration efforts. For the past two decades, SCC has been mainly used for bridges, and for underwater and heavily reinforced concrete structures. In the recent years, however, the use of SCC has been extended to building construction (Okamura, 1997).

SCC consists of the same components as conventional concrete (CC) cement, water, aggregates, admixtures, and mineral additions, but the final composition of the mixture and its fresh characteristics are different. Compared with CC, SCC contains larger quantities of mineral fillers such as finely crushed limestone or fly ash, as well as higher quantities of high-range water-reducing admixtures, and the maximum size of the coarse aggregate is smaller. These modifications in the composition of the mixture affect the properties of the concrete in its hardened state. Also, fresh properties and properties during hardening (e.g. hydration process) are influenced by the modifications in the composition. Using SCC can result in labour and cost savings,

but the increasing application of SCC requires a more precise understanding of its behaviour and performance. It is crucial to estimate the mechanical properties of this structural material accurately. The compressive and tensile strength of concrete is considered the most basic and important material property in designing concrete structures (Aslani and Nejadi, 2012a, 2012b, 2012c, 2012d).

The incorporation of fibres improves engineering performance of structural and non-structural concrete. The use of fibre-reinforced concrete (FRC) is also of special interest for retrofit and seismic design. The incorporation of metallic fibres can be problematic on some situations, especially when the fibre volume is high and the FRC is cast in sections with a moderate-to-high degree of reinforcement. The fibre content, length, aspect ratio and shape play an important role in controlling workability of FRC. Such concrete presents greater difficulty in handling, and requires more deliberate planning and workmanship than established concrete construction procedures. The additional compaction effort required for such concrete contributes to the increase in construction cost. In order to provide sufficient compaction, improve fibre dispersion, and reduce the risk of entrapping voids, the FRC is often proportioned to be fluid enough to reduce the need for vibration consolidation and facilitate placement. An extension of this approach can involve the use of SCC to eliminate, or greatly reduce, the need for vibration and further facilitate placement. A truly fibre-reinforced self-compacting concrete (FRSCC) should spread into place under its own weight and achieve consolidation without internal or external vibration, ensure proper dispersion of fibres, and undergo minimum entrapment of air voids and loss of homogeneity until hardening. Lack of proper self-compaction or intentional vibration and compaction can result in macro- and micro-structural defects that can affect mechanical performance and durability (Aslani and Nejadi, 2012e; Khayat and Roussel, 1999).

A few studies have been carried out on optimisation of the mix proportion for the addition of steel or polypropylene fibres to SCC. Meanwhile, there is insufficient research on the mechanical properties of FRSCC. In mechanical terms, the greatest disadvantage of cementitious material is its vulnerability to cracking, which generally occurs at an early age in concrete structures or members. Cracking may potentially reduce the lifetime of concrete structures and cause serious durability and serviceability problems. The addition of fibres into SCC mixtures has been studied by a number of researchers.

The standard concrete cylinders' (150×300 mm) compressive strength is regarded for design purposes as the basic material property. However, the common concept is that the concrete compressive strength value is incorrect because the compressive strength of concrete changes based on the specimen's size and shape. The size and shape of test specimens used to determine the compressive strength of concrete differ from country to country; nevertheless, the most commonly used specimens are cylinders and cubes. Cylinders (150×300 mm) are used in the USA, South Korea, France, Canada and Australia, among others, whereas cubes (150 mm) are the standard specimens used in the UK, Germany and most other European countries. Several countries (e.g. Norway) perform tests on both cylinders and cubes. Owing to differences in the shape and size, cylinder and cube strengths obtained from the same batch of concrete can differ (Yi *et al.*, 2006). Cubes usually have a higher strength than cylinders.

Since the early 1900s, many studies (Aïtcin *et al.*, 1994; Carrasquillo *et al.*, 1981; Chin *et al.*, 1997; Date and Schnormeier, 1981; Day and Haque, 1993; Lessard *et al.*, 1993; Malhotra, 1976; Moreno, 1990; Nasser and Kenyon, 1984; Neville, 1995; Sleiman *et al.*, 2000; Tokyay and Özdemir, 1997) in this field have been carried out. Most researchers have focused on developing guidelines for converting the compressive strength of concrete determined from nonstandard specimens to that of standard specimens. Many studies also investigated the relationship between cylinder strength and cube strength for CC. Generally, a factor of 1·2 is used to convert cylinder strength to cube strength for CC. However, the factor gradually decreases as the concrete strength increases. The CEB-FIP code 1990 (CEB-FIP, 1993) also indicates that the ratio of the cube strength to cylinder strength with increasing compressive strength of concrete decreases progressively from 1·25 to 1·12. The ratios 1·25 and 1·12 correspond to cylinder compressive strengths of 40 and 80 MPa, respectively.

In this study, the effect of specimen sizes and specimen shapes on compressive and tensile strengths of SCC specimens with and without fibres is experimentally investigated based on fracture mechanics. Also, it postulates the relationship for the prediction of compressive and tensile strengths based on specimen size. Furthermore, to obtain the concrete compressive strength of cylinders from specimens of other shapes, it theorises relationships generally applicable to both specimen shapes (i.e. cylinders and cubes). Developing a formula for converting the strength of cubes into the strength of cylinders could be of considerable interest to designers.

Experimental study

The experimental programme consisted of 30 cube specimens with 100 and 150 mm dimensions, and 30 cylinder specimens with 100×200 mm and 150×300 mm dimensions. Also, it examined four SCC mixtures: plain SCC, and steel-, polypropylene- and hybrid-fibre reinforced SCC. Compressive and tensile strengths were tested after 3, 7, 14, 28 and 56 days.

Properties of materials used in SCC and FRSCC

Cement

In this experimental study, shrinkage limited cement (SLC) corresponding to the AS 3972 (SA, 2010) standard was used. SLC is manufactured from specially prepared Portland cement clinker and gypsum. It may contain up to 5% of AS 3972-

approved additions. The chemical, physical and mechanical properties of the cement used in the experiments are shown in Table 1. The chemical, physical and mechanical properties adhere to the limiting value or permissible limits specified in AS 2350.2, 3, 4, 5, 8 and 11 (SA, 2006).

Fly ash

It is important to increase the amount of paste in SCC because fly ash is an agent that carries the aggregates. As a consequence, eraring fly ash (EFA) has been used to increase the amount of paste. EFA is a natural pozzolan. It is a fine cream/grey powder that is low in lime content. However, in its finely divided form and in the presence of moisture it will react chemically with calcium hydroxide (e.g. from lime or cement hydration) at ordinary temperatures to form insoluble compounds possessing cementitious properties. The chemical and physical properties of EFA used in the experimental study are given in Table 2. The chemical, physical and mechanical properties of the EFA used adhere to the limiting value or permissible limits specified in AS 2350.2 (SA, 2006), AS 3583.1, 2, 3, 5, 6, 12 and 13 (SA, 1998).

Ground granulated blast furnace slag

Ground granulated blast furnace slag (GGBFS) is another supplementary cementitious material that is used in combination with SLC. GGBFS used in the experiment originated in Boral, Sydney, and it conformed to AS 3582.2 (SA, 2001) specifications. The chemical and physical properties of GGBFS are given in Table 3.

Chemical properties	
Calcium oxide	64·5%
Silicon dioxide	19·3%
Aluminium oxide	5·2%
Iron (III) oxide	2·9%
Magnesium oxide	1·1%
Sulfur trioxide	2·9%
Potassium oxide	0·56%
Sodium oxide	<0·01%
Chloride ion	0·02%
Loss on ignition	2·8%
Physical properties	
Autoclave expansion	0·05%
Fineness index	405 m^2/kg
Mechanical properties	
Initial setting time	90 min
Final setting time	135 min
Soundness	1·0 mm
Drying shrinkage	590 μstrain
f'_c (3 days)	37·2 MPa
f'_c (7 days)	47·3 MPa
f'_c (28 days)	60·8 MPa

Table 1. Properties of cement

Chemical properties	
Aluminium oxide	26·40%
Calcium oxide	2·40%
Iron (III) oxide	3·20%
Potassium oxide	1·55%
Magnesium oxide	0·60%
Manganese oxide	<0·1%
Sodium oxide	0·47%
Phosphorus pentoxide	0·20%
Silicon dioxide	61·40%
Sulfur trioxide	0·20%
Strontium oxide	<0·1%
Titanium oxide	1·00%
Physical properties	
Moisture	<0·1%
Fineness 45 micron	78% passed
Loss on ignition	2·30%
Sulfuric anhydride	0·20%
Alkali content	0·50%
Chloride ion	<0·001%
Relative density	2·02%
Relative water requirement	97%
Relative strength 28 days	88%

Table 2. Properties of fly ash

Aggregate

In this study, crushed volcanic rock (i.e. latite) coarse aggregate was used with a maximum aggregate size of 10 mm. Nepean river gravel with a maximum size of 5 mm and Kurnell natural river sand fine aggregates were also used. The sampling and testing of aggregates were carried out in accordance with AS 1141 (SA, 2011) and the Regional Transportation Authority (RTA, 2006), and the results for coarse and fine aggregates are shown in Tables 4–6 respectively.

Chemical properties	
Aluminium oxide	14·30%
Iron (III) oxide	1·20%
Magnesium oxide	5·40%
Manganese oxide	1·50%
Sulfur trioxide	0·20%
Chloride ion	0·01%
Insoluble residue	0·50%
Loss on ignition	−1·10%
Physical properties	
Fineness index	435 m^2/kg

Table 3. Properties of ground granulated blast furnace slag

Characteristics	Results
Sieve size	Passing (%)
13·2 mm	100
9·5 mm	89
6·7 mm	40
4·75 mm	7
2·36 mm	1
1·18 mm	1
Material finer than 75 micron: %	1
Misshapen particles: %	
Ratio 2:1	13
Ratio 3:1	1
Flakiness index: %	20
Uncompacted bulk density: t/m^3	1·36
Compacted bulk density: t/m^3	1·54
Moisture condition of the aggregate: %	1·3
Particle density (dry): t/m^3	2·65
Particle density (SSD): t/m^3	2·70
Apparent particle density: t/m^3	2·79
Water absorption: %	1·9
Ave. dry strength: kN	391
Ave. wet strength: kN	293
Wet/dry strength variation: %	25
Test fraction: mm	−9·5 + 6·7
The amount of significant breakdown: %	<0·2
The size of testing cylinder = 150 mm diam.	
Los Angeles value grd. 'K': %loss	13

SSD: saturated-surface-dry.

Table 4. Properties of crushed latite volcanic rock coarse aggregate

Characteristics	Results
Sieve size	Passing (%)
6·7 mm	100
4·75 mm	99
2·36 mm	83
1·18 mm	64
600 micron	42
425 micron	28
300 micron	19
150 micron	8
Material finer than 75 micron: %	3
Uncompacted bulk density: t/m^3	1·52
Compacted bulk density: t/m^3	1·64
Particle density (dry): t/m^3	2·58
Particle density (SSD): t/m^3	2·60
Apparent particle density: t/m^3	2·63
Water absorption: %	0·7
Silt content: %	7
Degradation factor of fine aggregate	90
The wash water after using permitted 500 ml was: clear	
Moisture content: %	5·5
Method of determining voids content	
% voids	41·7
The mean flow time: s	26·5

SSD: saturated-surface-dry.

Table 5. Properties of Nepean river gravel fine aggregate

Characteristics	Results
Sieve size	Passing (%)
1·18 mm	100
600 micron	98
425 micron	87
300 micron	46
150 micron	1
Material finer than 75 micron in aggregate by washing: %	Nil
Uncompacted bulk density: t/m^3	1·39
Compacted bulk density: t/m^3	1·54
Particle density (dry): t/m^3	2·58
Particle density (SSD): t/m^3	2·59
Apparent particle density: t/m^3	2·62
Water absorption: %	0·6
Silt content: %	4

SSD: saturated-surface-dry.

Table 6. Properties of Kurnell natural river sand fine aggregate

Admixtures

The superplasticiser, viscosity-modifying admixture, and high-range water-reducing agent admixture were used in this study. The new superplasticiser generation Glenium 27 complies with AS 1478.1 (SA, 2000) type high range water reducer (HRWR) and ASTM C494 (ASTM, 2000) types A and F are used. The Rheomac VMA 362 viscosity modifying admixture that was used in this study is a ready-to-use, liquid admixture that is specially developed for producing concrete with enhanced viscosity and controlled rheological properties. Pozzolith 80 was used as a HRWR agent admixture in the mixes. It reduces the quantity of water required to produce concrete of a given consistency, with greater economy, of a given strength. It meets and exceeds AS 1478 (SA, 2000) type WRRe requirements for admixtures.

Fibres

In this study, two commercially available fibres, Dramix RC-80/60-BN type steel fibres and Synmix 65 type polypropylene (PP)

fibres, were used. The mechanical, elastic and surface structure properties of the steel and PP fibres are summarised in Table 7.

Mixture proportions

One control SCC mixture (N-SCC) and three fibre-reinforced SCC mixtures were used in this study. The fibre-reinforced SCC mixtures contained steel (D-SCC), PP (S-SCC), and hybrid (steel + PP) (DS-SCC) fibres. The content proportions of these mixtures are given in Table 8. These contents were chosen to attempt to keep compressive strength to a level applicable to construction.

Sample preparation and curing conditions

The dimensions and shapes used in the experiments for compressive strength are 30 cube specimens with 100 and 150 mm dimensions, and 30 cylinder specimens with 100×200 mm and 150×300 mm dimensions. Also, cylinder specimens with 100×200 mm and 150×300 mm dimensions were used for splitting tensile tests. The specimens were prepared by directly pouring concrete into moulds without compaction. The specimens were kept covered in a controlled chamber at 20 ± 2°C for 24 h until their demoulding. Thereafter, the specimens were placed in water presaturated with lime at 20°C. The compressive and tensile strengths were tested after 3, 7, 14, 28 and 56 days.

Properties of fresh concrete

The experiments required for the SCC are generally carried out worldwide under laboratory conditions. These experiments test the flowability, segregation, placement, and compacting of fresh concrete. Conventional workability experiments are not sufficient for the evaluation of SCC. Some of the experiment methods developed to measure the flowability, segregation, placement and compaction of SCC are defined in the European guidelines (EFNARC, 2005) and ACI 237R-07 (ACI, 2007) for SCC, including specification, production and use as slump–flow, V-funnel, U-box, L-box and fill-box tests.

Fibre type	Fibre name	Density: kg/m^3	Length (l): mm	Diameter (d): mm	Aspect ratio (l/d)	Tensile strength: MPa	Modulus of elasticity: GPa	Cross-section form	Surface structure
Steel	Dramix RC-80/60-BN	7850	60	0·75	80·0	1050	200	Circular	Hooked end
Polypropylene	Synmix 65	905	65	0·85	76·5	250	3	Square	Rough

Table 7. The physical and mechanical properties of fibres

Constituents	N-SCC	D-SCC	S-SCC	DS-SCC
Cement: kg/m^3	160	160	160	160
Fly ash: kg/m^3	130	130	130	130
GGBFS: kg/m^3	110	110	110	110
Cementitious content: kg/m^3	400	400	400	400
Water: litre/m^3	208	208	208	208
Water cementitious ratio	0·52	0·52	0·52	0·52
Fine aggregate: kg/m^3				
Coarse sand	660	660	660	660
Fine sand	221	221	221	221
Coarse aggregate: kg/m^3	820	820	820	820
Admixtures: litre/m^3				
Superplasticiser	4	4·86	4·73	4·5
VMA	1·3	1·3	1·3	1·3
High range water reducing agent	1·6	1·6	1·6	1·6
Fibre content: kg/m^3				
Steel	—	30	—	15
PP	—	—	5	3

GGBFS: ground granulated blast furnace slag; PP: polypropylene.

Table 8. The proportions of the concrete mixtures (based on SSD condition)

This study performed slump flow, T_{50cm} time, J-ring flow, V-funnel flow time and L-box blocking ratio tests. In order to reduce the effect of loss of workability on the variability of test results, the fresh properties of the mixes were determined within 30 min of mixing. The order of testing is as follows

- slump flow test and measurement of T_{50cm} time
- J-ring flow test, measurement of difference in height of concrete inside and outside the J-ring, and measurement of T_{50cm} time
- V-funnel flow tests at 10 s T_{10s}
- L-box test.

Experimental results

Properties of fresh concrete

The results of various fresh properties tested by the slump flow test (slump flow diameter and T_{50cm}); J-ring test (flow diameter); L-box test (time taken to reach 400 mm distance T_{400mm}, time taken to reach 600 mm distance T_{600mm}, time taken to reach 800 mm distance T_L and ratio of heights at the two edges of L-box [H_2/H_1]); V-funnel test (time taken by concrete to flow through V-funnel after 10 s T_{10s}); the amount of entrapped air; and the specific gravity of mixes are given in Table 9. The slump flow test judges the capability of concrete to deform under its own weight against the friction of the surface with no restraint present. A slump flow value ranging from 500 to 700 mm for SCC was suggested (EFNARC, 2005). At a slump flow $>$700 mm, the concrete might segregate, and at $<$500 mm, the concrete might have insufficient flow to pass through highly congested reinforcements. All the mixes in the present study conform to the above range because the slump flow of SCC is in the range of 600–700 mm. The slump flow time for the concrete to reach a diameter of 500 mm for all mixes was less than 4·5 s. The J-ring diameters were in the range of 560–655 mm. In addition to the slump flow test, a V-funnel test was also performed to assess the flowability and stability of SCC. V-funnel flow time is the elapsed time, in seconds, between the opening of the bottom outlet, depending when it is opened (T_{10s} and T_{5min}), and the time when light becomes visible at the bottom when observed from the top. A V-funnel time of less than 6 s is recommended for SCC. According to EFNARC (2005), a period ranging from 6 to 12 s is considered adequate for SCC.

The V-funnel flow times in the experiment were in the range of 7–11 s. The test results of this investigation indicated that all mixes met the requirements of allowable flow time. V-funnel flow time test results for the N-SCC mix was about 6 s and for the D-SCC was 7 s; for other fibre reinforced SCC mixes are blocked.

The maximum size of coarse aggregate was restricted to 10 mm to avoid a blocking effect in the L-box for N-SCC mix. The gap between rebars in the L-box test was 35 mm. The L-box ratio H_2/H_1 for the N-SCC mix was above 0·8, which is according to EFNARC standards and for other mixes is blocked.

Compressive and tensile strength results

Figure 1 shows the compressive strength experimental results for cube specimens with 100 and 150 mm dimensions, and for cylinder specimens with 100 × 200 and 150 × 300 mm dimensions. The tensile strength experimental results for cylinder specimens with dimensions of 100 × 200 and 150 × 300 mm are shown in Figure 1. In this figure, compressive and tensile strength results for all mixes are shown at the ages of 3, 7, 14, 28 and 56 days.

A general comparison of the compressive strengths of cubes of 100 and 150 mm shows that the DS-SCC mix had higher compressive strength than other mixes. Also, the N-SCC mix had the lowest compressive strength and the S-SCC mix had higher compressive strength than the D-SCC mixes (see Figures 1(a) and 1(b)). However, the comparisons of the compressive strengths of 150-mm cubes show that the N-SCC mix strength is 11·15% higher, the D-SCC mix is 9·16% higher, the S-SCC mix is 7·56% higher and the DS-SCC mix is 7·83% higher than the compressive strengths of 100-mm cubes.

Workability characteristics	ACI 237R-07 and EFNARC	N-SCC	D-SCC	S-SCC	DS-SCC
Average spreading diameter: mm	650–800	680	670	700	650
Flow time T_{50cm}: s	2·5–5	2·7	3·8	2·5	3·2
Average J-ring diameter: mm	650–800	655	580	570	560
Flow time T_{50cm} J-ring: s	2·5–5	3·2	5	6	5
L-box test	0·8–1·0	0·87	Blocked	Blocked	Blocked
Flow time V-funnel: s	6–12	6	7	Blocked	Blocked
Entrapped air: %	–	1·3	1·2	1·2	1·0
Specific gravity: kg/m^3	–	2340	2274	2330	2385

Table 9. The self-compacting concrete mixes workability characteristics

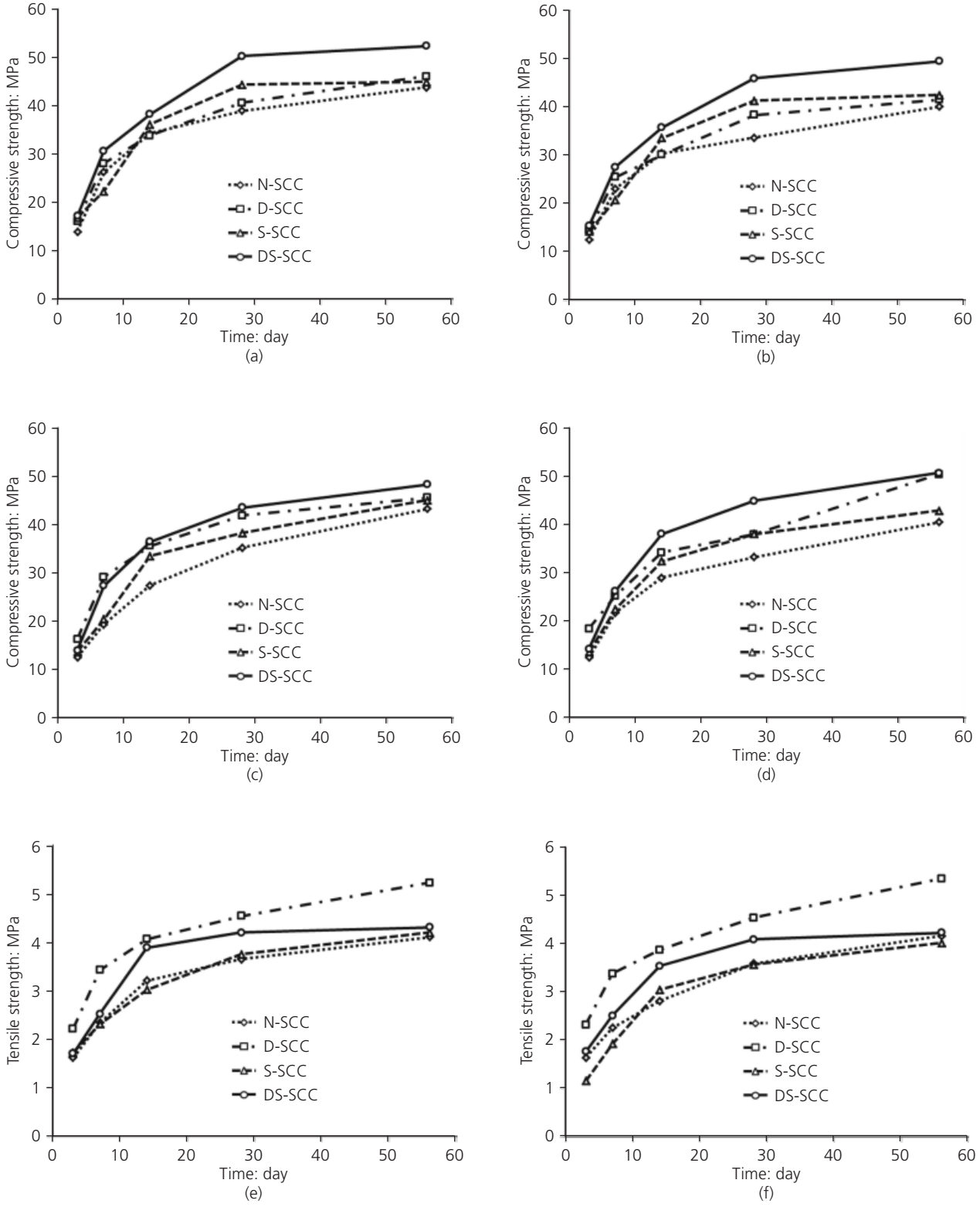

Figure 1. Compressive and tensile strengths (a) cube 100 mm, (b) cube 150 mm, (c) cylinder 100 × 200 mm, (d) cylinder 150 × 300 mm, (e) cylinder 100 × 200 mm and (f) cylinder 150 × 300 mm

Figures 1(c) and 1(d) show that DS-SCC has higher compressive strength than other mixes, and that S-SCC mix has the lowest compressive strength for 100×200 and 150×300-mm cylinders. The comparisons of the compressive strengths of 150×300 mm cylinders show that the N-SCC mix strength is 0·5% higher, the D-SCC mix is 1·22% higher, the S-SCC mix is 0·93% higher and the DS-SCC mix is 2·65% lower than the compressive strengths of 100×200 mm cylinders.

Figures 1(e) and 1(f) show that D-SCC has a higher tensile strength, and N-SCC and S-SCC have lower tensile strengths for 100×200 and 150×300 mm cylinders. The comparisons of the tensile strengths of 150×300 mm cylinders show that the N-SCC mix strength is 3·2% higher, the D-SCC mix is 0·16% higher the S-SCC mix is 8·8% higher and the DS-SCC mix is 3·1% lower than the tensile strengths of 100×200 mm cylinders.

Theoretical analysis

Theoretical analysis of the size effect

Bazant (1984) and Kim and Eo (1990) proposed the modified size effect law (MSEL; Equation 1) by adding the size independent strength $\sigma_o(=\alpha\ f_{ct})$ to the size effect law to predict the strength of concrete structures with or without initial cracks, and with similar or dissimilar cracks (Yi *et al.*, 2006). This concept was also proposed by Bazant (1987, 1993) and Bazant and Xiang (1997), with a different solution procedure

$$\sigma_N(d) = \frac{B\, f_{ct}}{\sqrt{1 + d/\lambda_o\, d_a}} + \alpha\, f_{ct} \quad (1)$$

where $\sigma_N(d)$ is the nominal strength; f_{ct} is the direct tensile strength; d is the characteristic dimension; d_a is the maximum aggregate size; and B, λ_o and α are the empirical constants.

Although the failure mechanism and effect of size on tensile failure have been studied extensively, the behaviour of compressive failure has not been sufficiently studied in comparison. Concrete is a construction material normally used to withstand compressive force. Accordingly, more studies in this field are necessary. As it is logical to extend the tensile size effect research to compressive failure research, the direct tensile strength f_{ct} used in the MSEL must be substituted with the compressive strength of standard cylinder f'_c in the new equation for the prediction of the effect of size on compression. This substitution can be done because, even though the tensile failure mechanism is different from the compressive failure mechanism, the ultimate failure of both is attributable to the propagation of macro-crack, indicating a localised tension or mode I failure. Therefore, it is safe to assume that the tensile fracture-based concept can be applied to compressive failure as well. The validity of the MSEL was demonstrated by regression analyses on available test data for tensile strength, shear strength and uniaxial compressive strength.

As an application of MSEL, some studies have been performed on unnotched and notched cylindrical specimens subjected to uniaxial compressive force; on axially loaded, double-cantilever beams; and on C-shaped specimens subjected to flexural compression force. In Equation 1, the width of crack band l_o is empirically found to be related to the maximum aggregate size d_a (in this study, $d_a = 10$ mm), for example $l_o = \lambda_o d_a$ in which λ_o is an approximate constant with values between 2·0 and 3·0 (Bazant, 1984; Kim *et al.*, 1999, 2000, 2001). In the regression analysis, this constant is selected as 2·0, where $l_o = 2{\cdot}0$ and $d_a = 20{\cdot}0$ mm. In a previous study (Kim *et al.*, 1999), Equation 2 was proposed to obtain the compressive strength of cylindrical concrete specimens with various diameters and height/diameter ratios. For this purpose, the effects of the maximum aggregate size on the fracture process zone were considered and the concept of characteristic length was newly introduced. The method to determine the characteristic length is derived and explained by Kim and Eo (1990).

$$\sigma_N(hd) = \frac{0{\cdot}4\, f'_c}{\sqrt{1 + (h-d)/5}} + 0{\cdot}8\, f'_c \quad (2)$$

where the height of cylinder specimen h and the diameter of cylinder specimen d are in cm. Equation 2 was compared with the ASTM standard (ASTM, 2000), and it was noted that the prediction values of Equation 2 are less than those of the ASTM standard, but the difference is minimal.

Size effect for cubes

Figure 2 shows the value $f'_{cmu}(d)/f'_c$ ($f'_{cmu}(d)$ is the compressive strength of cube and f'_c is the N-SCC mix compressive strength) as a function of the specimen size d and the strong size effect for compressive strengths of cubes. Regression analyses were conducted to measure the compressive strength of the cubes, Equations 3–6 were obtained, and the results were graphed and are shown in Figure 2.

For N-SCC

$$f'_{cmu}(d) = \frac{1{\cdot}3\, f'_c}{\sqrt{1 + d/l_o}} + 0{\cdot}62\, f'_c \quad (3)$$

For D-SCC

$$f'_{cmu}(d) = \frac{1{\cdot}3\, f'_{cfD}}{\sqrt{1 + d/l_o}} + 0{\cdot}62\, f'_{cfD} \quad (4)$$

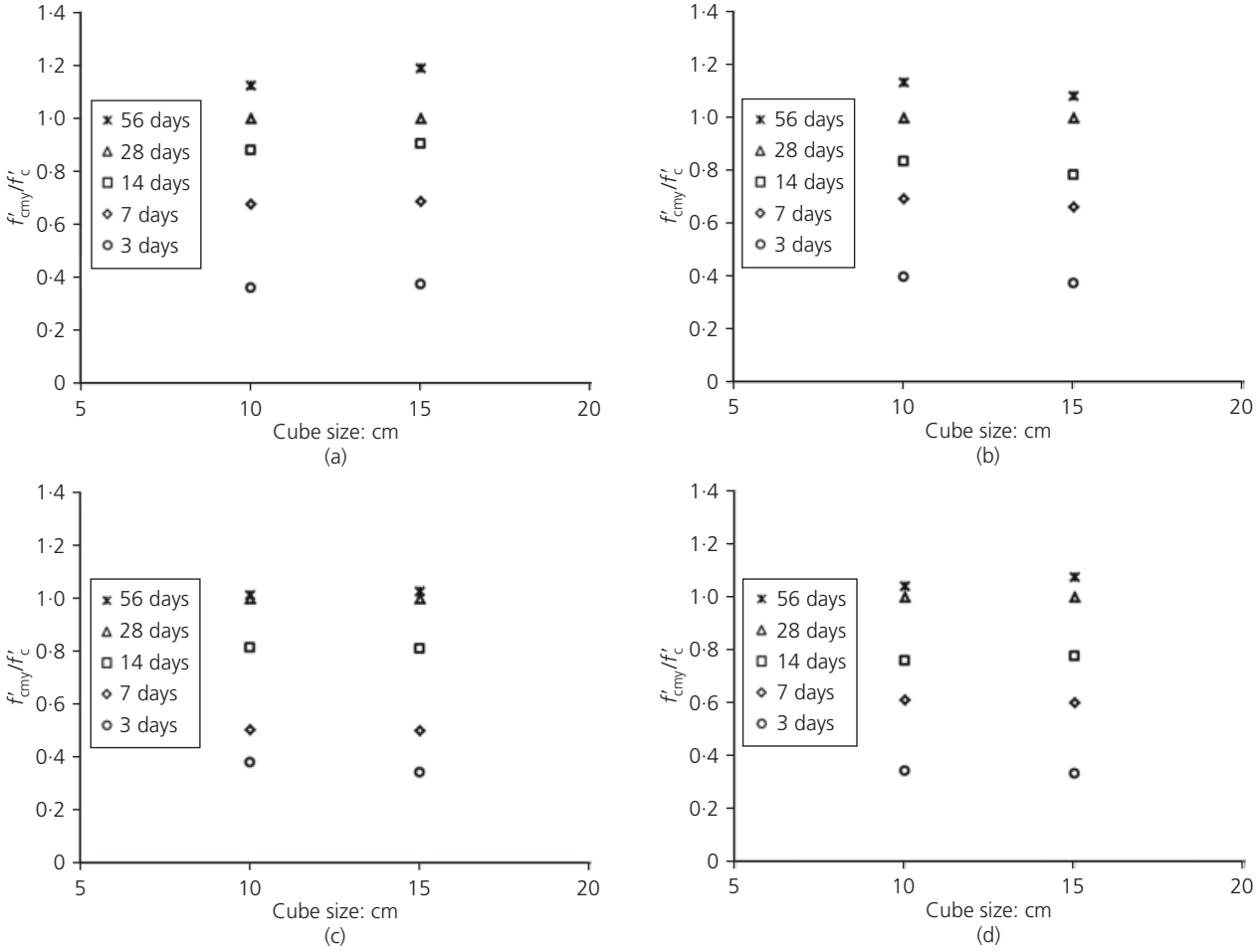

Figure 2. Compressive strength size effect for cubes (a) N-SCC, (b) D-SCC, (c) S-SCC and (d) DS-SCC

For S-SCC

$$5.\quad f'_{cmu}(d) = \frac{1{\cdot}3\, f'_{cfS}}{\sqrt{1 + d/l_o}} + 0{\cdot}62\, f'_{cfS}$$

For DS-SCC

$$6.\quad f'_{cmu}(d) = \frac{1{\cdot}3\, f'_{cfDS}}{\sqrt{1 + d/l_o}} + 0{\cdot}62\, f'_{cfDS}$$

where f'_{cfD} is the D-SCC mix compressive strength, f'_{cfS} is the S-SCC mix compressive strength and f'_{cDS} is the DS-SCC mix compressive strength in MPa; the size of the cube d is in cm, $l_o = 2{\cdot}0d_a$ and d_a is the maximum aggregate size. The compressive strengths for the D-SCC, S-SCC and DS-SCC mixes were obtained based on the regression analyses as shown in Equations 7–9.

For D-SCC

$$7.\quad f'_{cfD} = f'_c + 15{\cdot}2\,(\text{R.I.})$$

For S-SCC

$$8.\quad f'_{cfS} = f'_c - 3\,(\text{R.I.})$$

For DS-SCC

$$9.\quad f'_{cfDS} = f'_c + 12{\cdot}85\,(\text{R.I.})$$

where the R.I. is the fibre reinforcing index ($= V_f \times l_f/d_f$), fibre volume fractions (V_f) and aspect ratio (l_f/d_f).

Size effect for compressive strength cylinder

Equations 10–13 were obtained from least squares method regression analyses for cylinders. Figure 3 shows the value $f'_{cmy}(d)/f'_c$ ($f'_{cmy}(d)$ is the compressive strength with size of general cylinder) as a function of the diameter d. In this study, it is concluded that the strength ratio approaches a limit with an increasing diameter d.

For N-SCC

$$f'_{cmy}(d) = \frac{0{\cdot}55\, f'_c}{\sqrt{1 + d/l_o}} + 0{\cdot}81\, f'_c \quad (10)$$

For D-SCC

$$f'_{cmy}(d) = \frac{0{\cdot}55\, f'_{cfD}}{\sqrt{1 + d/l_o}} + 0{\cdot}81\, f'_{cfD} \quad (11)$$

For S-SCC

$$f'_{cmy}(d) = \frac{0{\cdot}55\, f'_{cfS}}{\sqrt{1 + d/l_o}} + 0{\cdot}81\, f'_{cfS} \quad (12)$$

For DS-SCC

$$f'_{cmy}(d) = \frac{0{\cdot}55\, f'_{cfDS}}{\sqrt{1 + d/l_o}} + 0{\cdot}81\, f'_{cfDS} \quad (13)$$

where the N-SCC mix compressive strength f'_c, the D-SCC mix compressive strength f'_{cfD} (Equation 7), the S-SCC mix compressive strength f'_{cfS} (Equation 8) and the DS-SCC mix compressive strength f_{cfDS} (Equation 9) are in MPa, and size of the cylinder d is in cm, where $l_o = 2{\cdot}0d_a$, and d_a is the maximum aggregate size. The term 'general' represents the cylinders with arbitrary chosen dimensions.

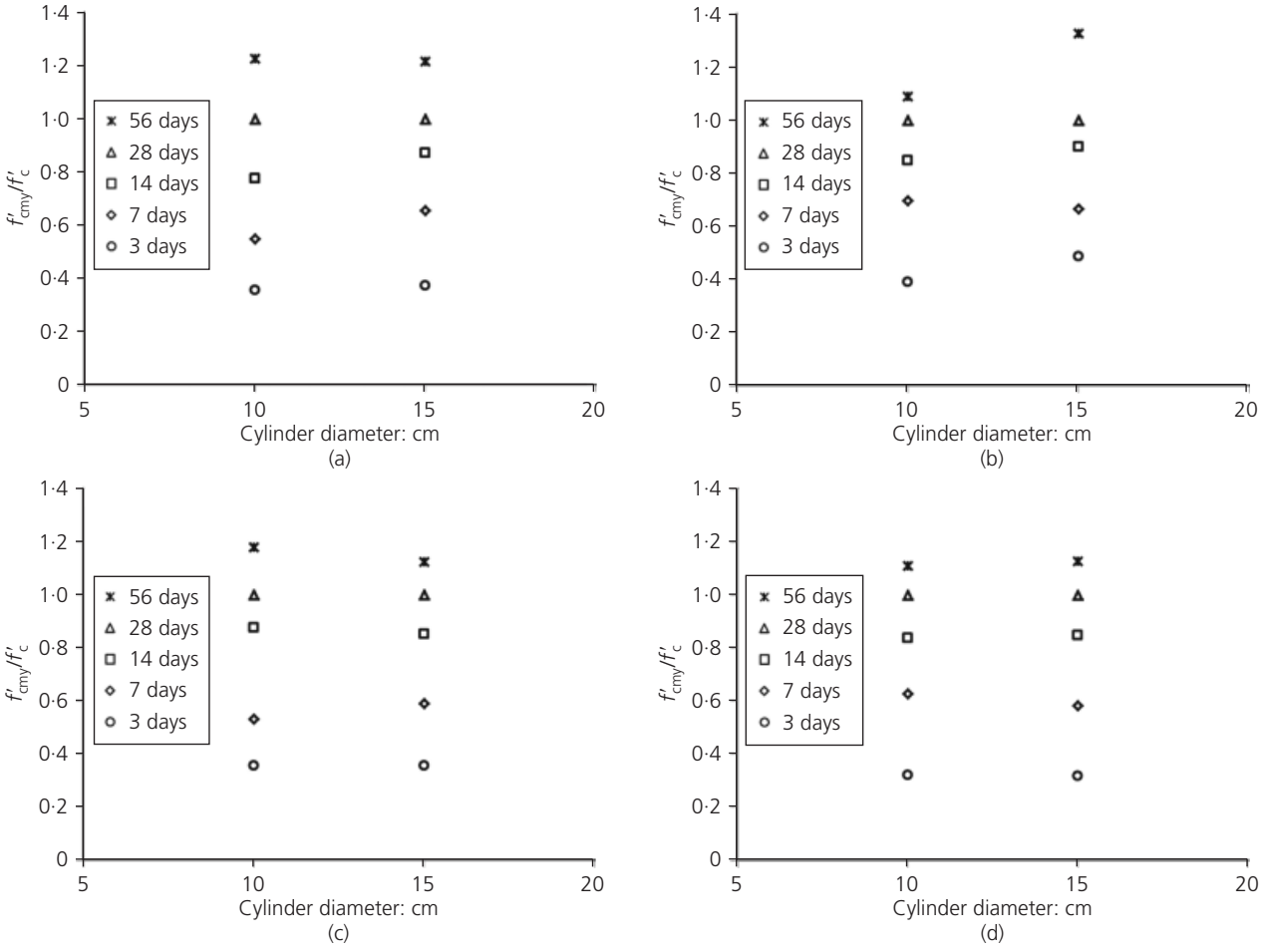

Figure 3. Compressive strength size effect for cylinders
(a) N-SCC, (b) D-SCC, (c) S-SCC and (d) DS-SCC

Size effect for tensile strength cylinder

Figure 4 shows the value $f_{ctmy}(d)/f_{ct}$ ($f_{ctmy}(d)$ is the tensile strength of cylinder and f_{ct} is the N-SCC mix tensile strength) as a function of the specimen size d and the strong size effect for tensile strengths of cubes. Regression analyses were conducted to measure the tensile strengths of the cubes, Equations 14–17 were obtained, and the results were graphed and are shown in Figure 4.

For N-SCC

$$f_{\text{ctmy}}(d) = \frac{0{\cdot}8\, f_{\text{ct}}}{\sqrt{1 + d/l_{\text{o}}}} + 0{\cdot}72\, f_{\text{ct}} \quad (14)$$

For D-SCC

$$f_{\text{ctmy}}(d) = \frac{0{\cdot}8\, f_{\text{fctD}}}{\sqrt{1 + d/l_{\text{o}}}} + 0{\cdot}72\, f_{\text{fctD}} \quad (15)$$

For S-SCC

$$f_{\text{ctmy}}(d) = \frac{0{\cdot}8\, f_{\text{fctS}}}{\sqrt{1 + d/l_{\text{o}}}} + 0{\cdot}72\, f_{\text{fctS}} \quad (16)$$

For DS-SCC

$$f_{\text{ctmy}}(d) = \frac{0{\cdot}8\, f_{\text{fctDS}}}{\sqrt{1 + d/l_{\text{o}}}} + 0{\cdot}72\, f_{\text{fctDS}} \quad (17)$$

where the D-SCC mix tensile strength f_{fctD}, the S-SCC mix tensile strength f_{fctS} and the DS-SCC mix tensile strength f_{fctDS} are in MPa, and the size of the cylinder d is in cm, where $l_{\text{o}} = 2{\cdot}0d_{\text{a}}$ and d_{a} is the maximum aggregate size. The tensile strength for the D-SCC, S-SCC and DS-SCC mixes were obtained based on the regression analyses as shown in Equations 18–20.

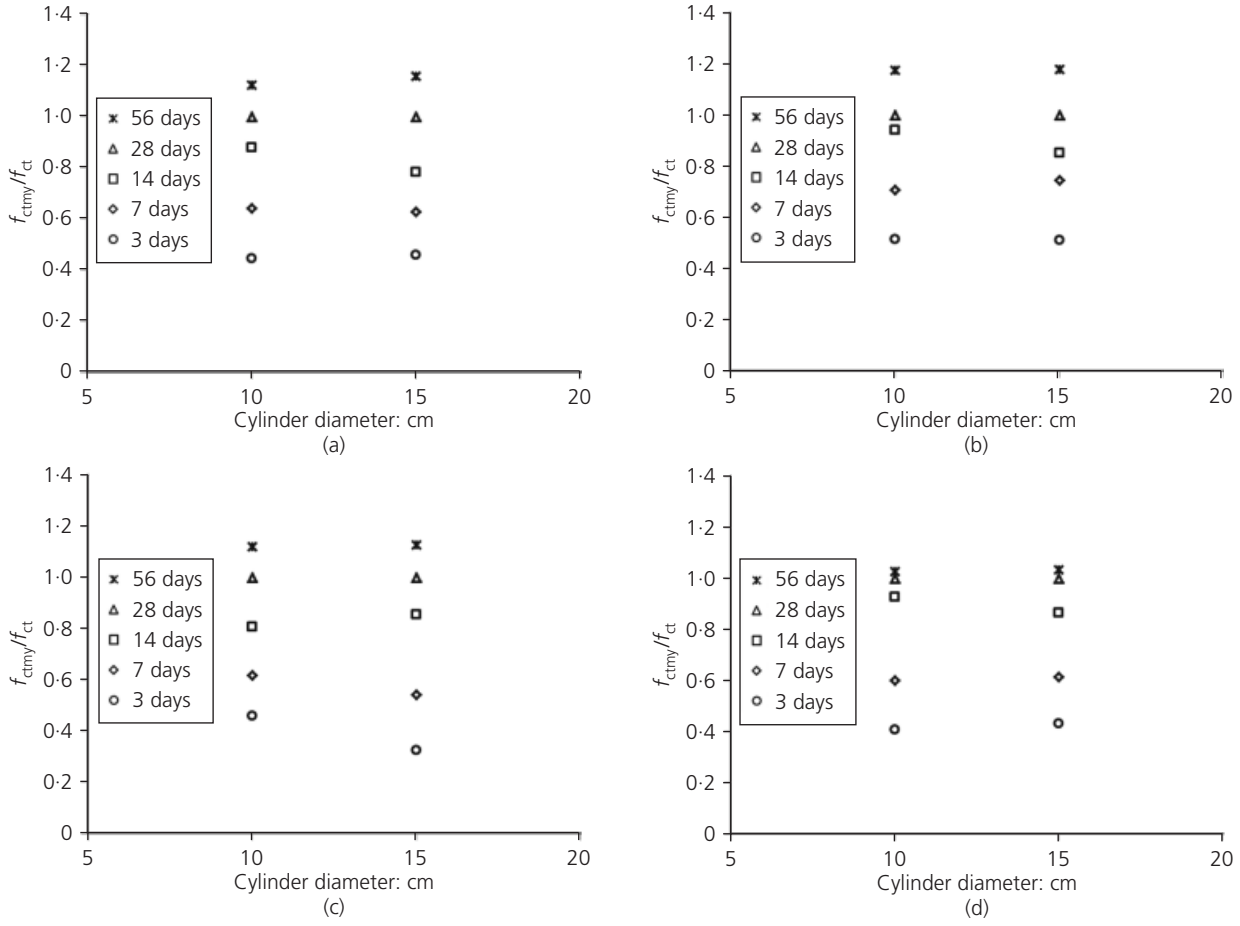

Figure 4. Tensile strength size effect for cylinders (a) N-SCC, (b) D-SCC, (c) S-SCC and (d) DS-SCC

For D-SCC

$$f_{\mathrm{fctD}} = f_{\mathrm{ct}} + 5{\cdot}1\,(\mathrm{R.I.}) \quad (18)$$

For S-SCC

$$f_{\mathrm{fctS}} = f_{\mathrm{ct}} - 3\,(\mathrm{R.I.}) \quad (19)$$

For DS-SCC

$$f_{\mathrm{fctDS}} = f_{\mathrm{ct}} + 4{\cdot}3\,(\mathrm{R.I.}) \quad (20)$$

where the R.I. is the fibre reinforcing index ($= V_{\mathrm{f}} \times l_{\mathrm{f}}/d_{\mathrm{f}}$), fibre volume fractions (V_{f}) and aspect ratio ($l_{\mathrm{f}}/d_{\mathrm{f}}$).

Relationship between specimen shapes

Figures 5–8 show plot the cylinders' against the cubes' compressive strengths for the represented specimen sizes. In these figures, solid lines and dashed lines indicate the best-fit lines obtained from linear regression analyses and the lines of equality $Y = X$ respectively. In addition, the equations shown in Figures 5–8 are achieved from linear regression analyses with test data points. The 100×200 mm cylinder strength, when plotted against the corresponding 100 mm cube strength, is shown in Figure 5. Figures 5(a), 5(c) and 5(d) show that the 100 mm cube strength is higher for N-SCC, S-SCC and DS-SCC. Figure 5(b) shows that the 100 mm cube strength is a bit lower than the 100×200 mm cylinder strength for D-SCC.

The 100×200 mm cylinder strength, when plotted against the corresponding 150 mm cube strength, is shown in Figure 6. Figure 6(a) shows that cube strength is higher for lower grades of

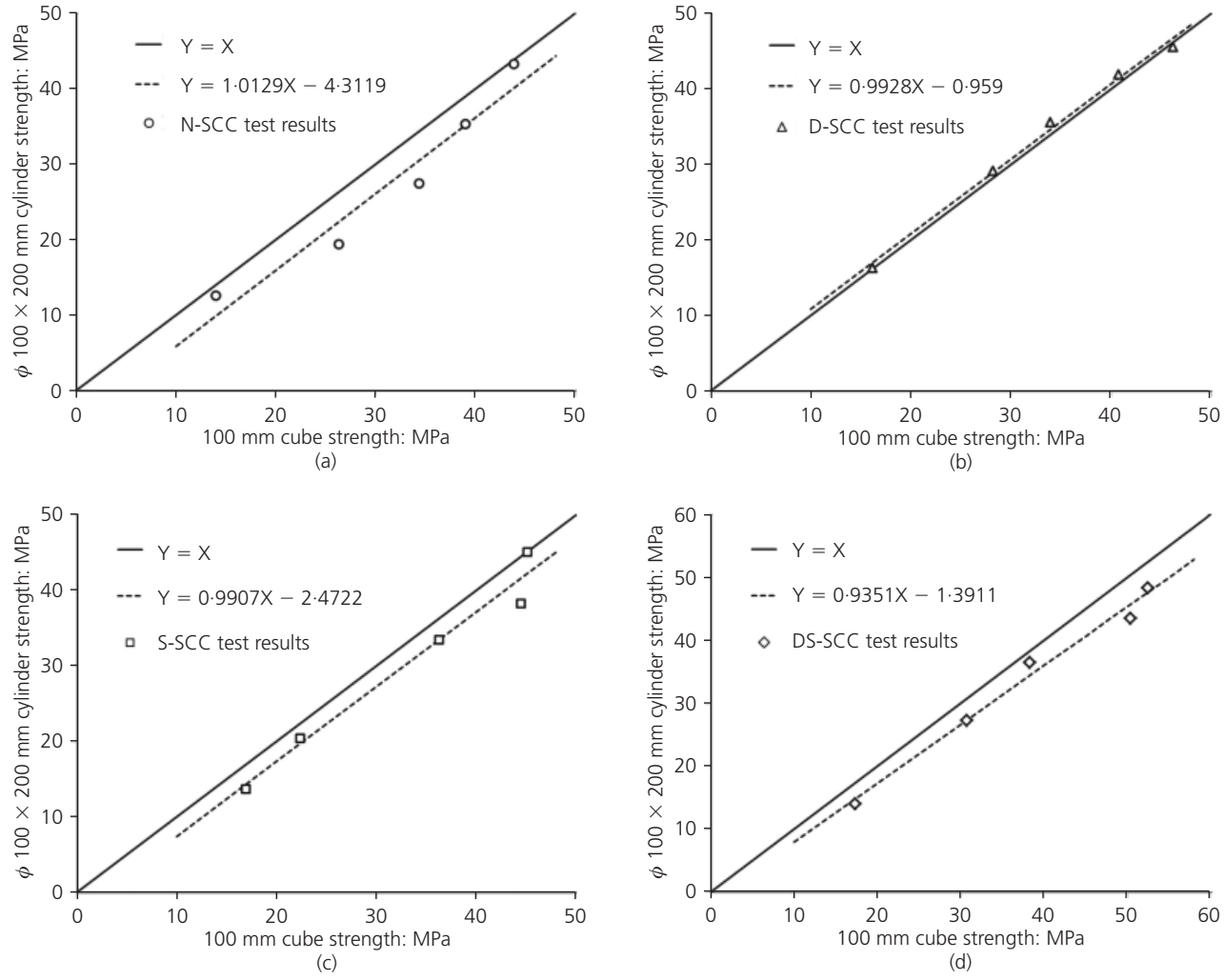

Figure 5. Relationship between compressive strengths of the 100×200 mm cylinder and the 100 mm cube. (a) N-SCC, (b) D-SCC, (c) S-SCC and (d) DS-SCC

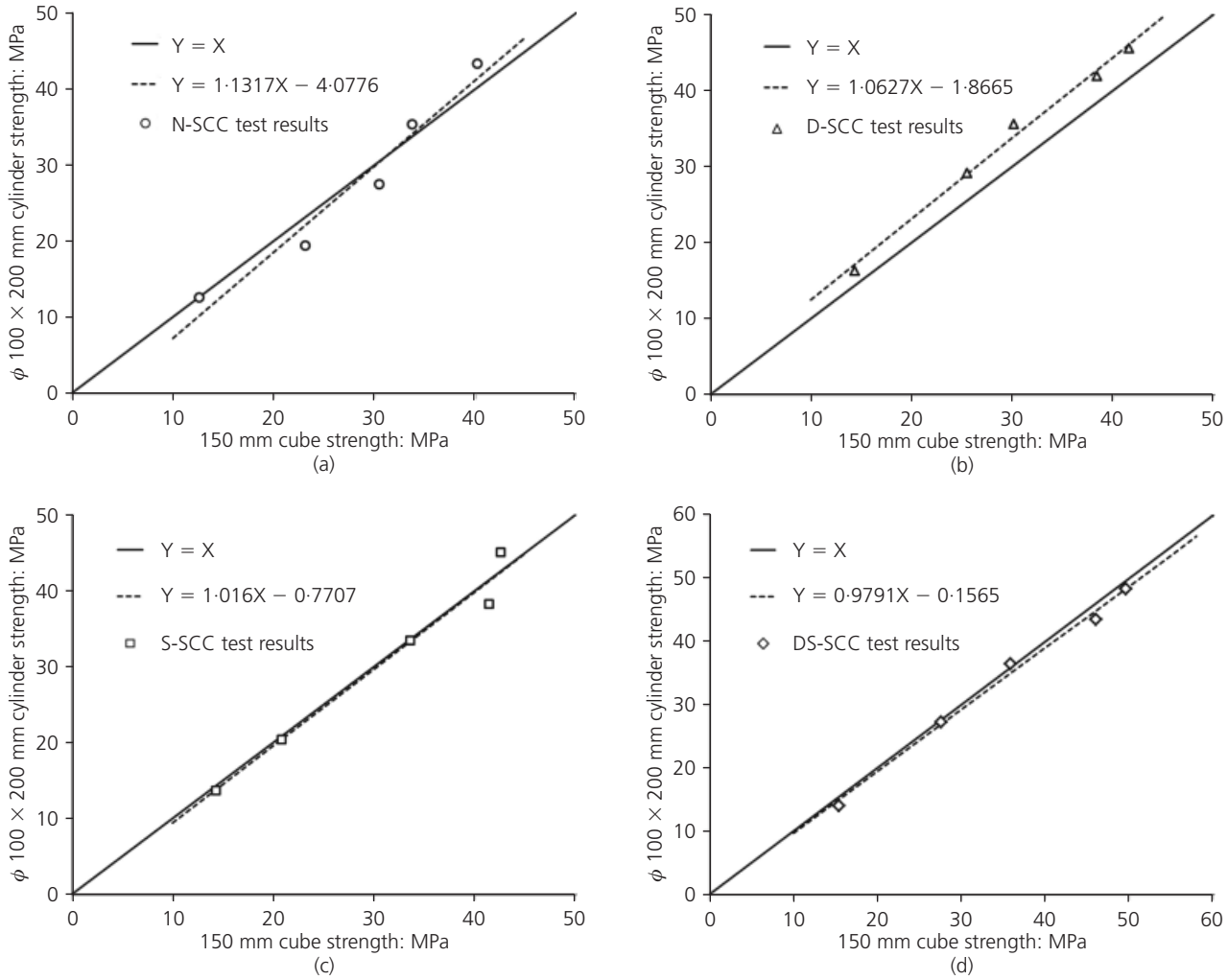

Figure 6. Relationship between compressive strengths of the 100 × 200 mm cylinder and the 150 mm cube. (a) N-SCC, (b) D-SCC, (c) S-SCC, and (d) DS-SCC

N-SCC. At approximately 30 MPa, however, the strengths become identical. Beyond that point, standard cylinders indicate a slightly higher strength than corresponding cubes do. Figures 6(c) and 6(d) show that the 150 mm cube strength is nearly identical for the S-SCC and DS-SCC mixes. Figure 5(b) shows that the 150 mm cube strength is lower than the 100 × 200 mm cylinder strength for D-SCC. The 150 × 300 mm cylinder strength, when plotted against the corresponding 100 mm cube strength, is shown in Figure 7. Figures 7(a), 7(c) and 7(d) show that the 100 mm cube strength is higher for the N-SCC, S-SCC and DS-SCC mixes. Figure 7(b) shows that the 100 mm cube strength is identical to the 100 × 200 mm cylinder strength for D-SCC.

The 150 × 300 mm cylinder strength, when plotted against the corresponding 150 mm cube strength, is shown in Figure 8. Figures 8(a) and 8(d) show that the 150 mm cube strength is nearly identical for N-SCC and DS-SCC mixes. Figure 8(b) shows that the 150 mm cube strength is lower than the 150 × 300 mm cylinder strength for D-SCC. Figure 8(c) shows that cube strength is higher for lower grades of S-SCC. At approximately 250 MPa, however, the strengths became identical. Beyond that point, standard cylinders indicated a slightly higher strength than the corresponding cubes did.

Conclusions

Conclusions can be drawn from this experimental and theoretical study, as outlined below.

- Size effect based on the specimen size and shape difference is present for SCC and FRSCC mixes.
- The effect of size on cubes is greater than that on cylinders for all the examined SCC mixes.

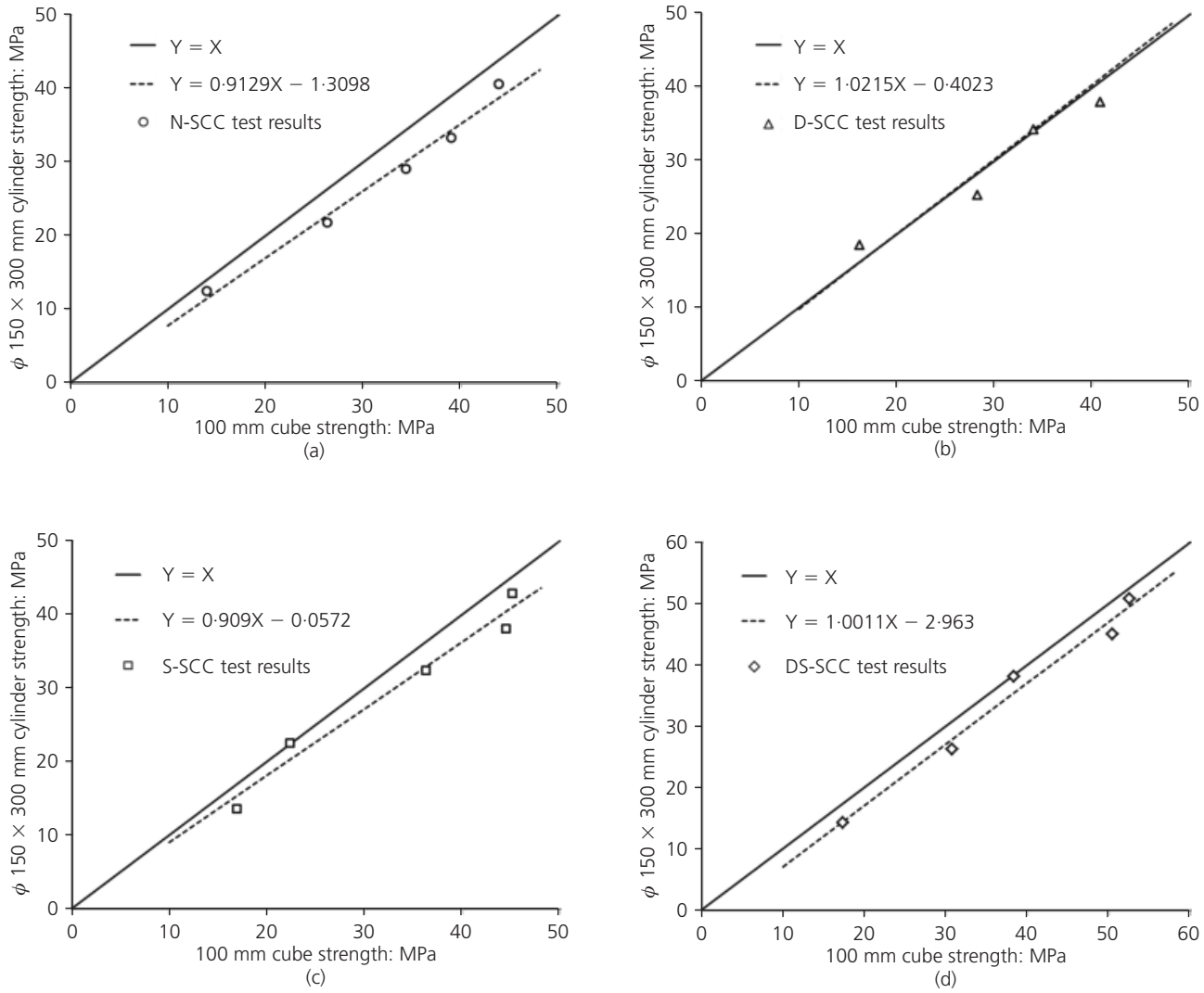

Figure 7. Relationship between compressive strengths of the 150 × 300 mm cylinder and the 100 mm cube. (a) N-SCC, (b) D-SCC, (c) S-SCC and (d) DS-SCC

- The DS-SCC mix has a higher compressive strength than the other mixes in all specimens. Additionally, the D-SCC mix has a higher tensile strength than the other mixes for 100 × 200 mm (3·93 × 7·87 in) and 150 × 300 mm (5·90 × 11·81 in) cylinders.
- To obtain the concrete compressive and tensile strengths, the relationships of the size effect for cubes and for cylinders were suggested based on fracture mechanics. Furthermore, these relationships are applicable to N-SCC, D-SCC, S-SCC and DS-SCC.
- The proposed relationship of the size effect for cubes and for compressive and tensile cylinders begins with the same principle. However, in reinforced SCC mixtures, the compressive and tensile strength equations are different; this phenomenon is related to the compressive and tensile strength of N-SCC and the fibre reinforcing index.
- The presented test results show the existence of a shape effect. Shape effect analyses show that the cube's strength is lower or nearly equal to the cylinder's strength for D-SCC mix for all dimensions. Furthermore, these analyses illustrated that the cube's strength is higher or nearly identical to the cylinder's strength for N-SCC, S-SCC and DS-SCC for all dimensions.
- The proposed relationships are useable for FRSCC and normal SCC. However, the main parameter that should be calibrated based on the new mix design or different using fibre type is general compressive strength ($f'_{c,i}$ and $f'_{c,ii}$) for cube, cylinder specimens and general tensile strength($f_{ct,i}$)

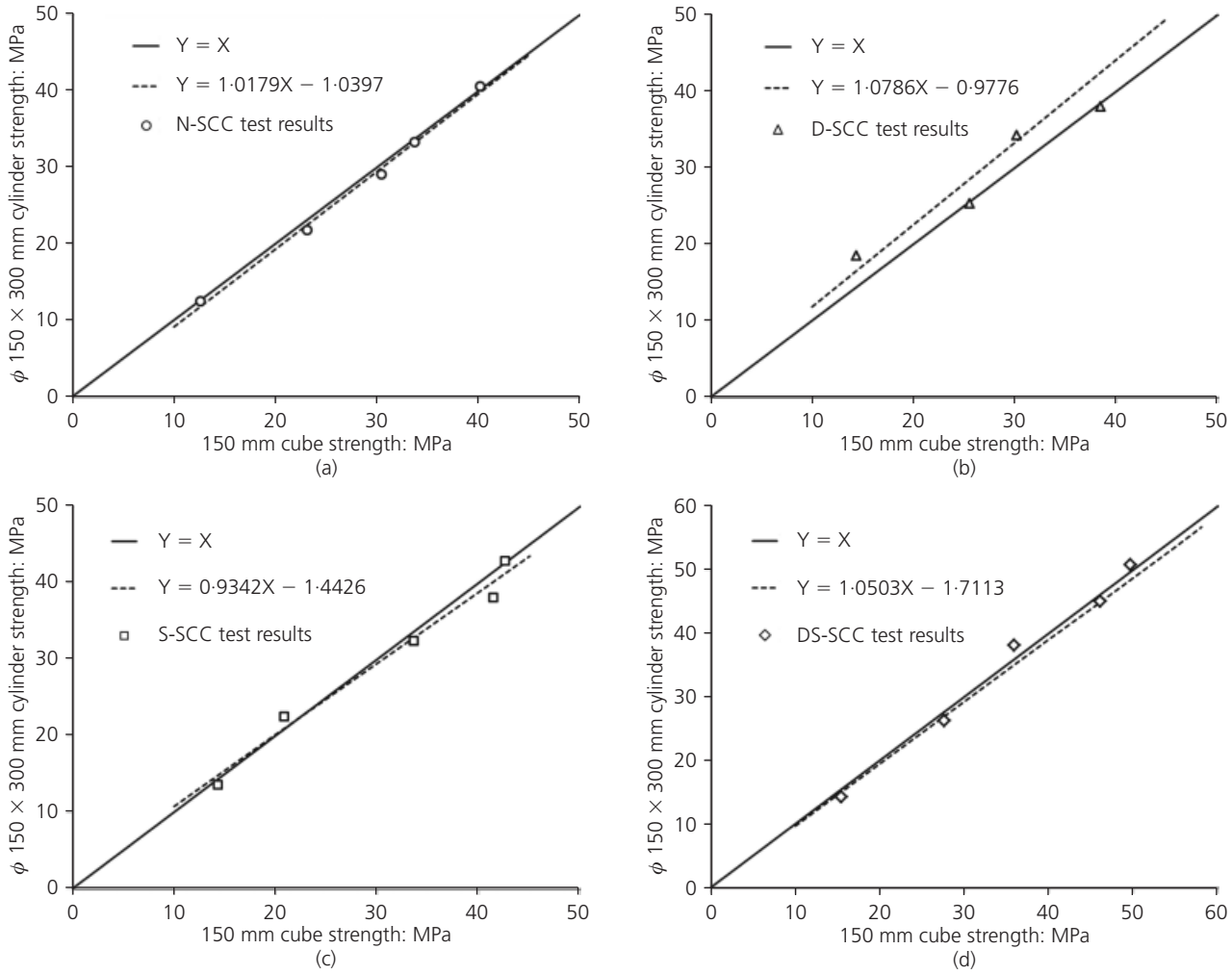

Figure 8. Relationship between compressive strengths of the 150 × 300 mm cylinder and the 150 mm cube. (a) N-SCC, (b) D-SCC, (c) S-SCC and (d) DS-SCC

for cylinder specimens. By calibrating this parameter the presented relationships and results in this study are useful for variable SCC investigations.

REFERENCES

ACI (American Concrete Institute) (2007) ACI 237R-07. Self-consolidating concrete. ACI Committee 237. ACI, Farmington Hills, MI, USA.

Aïtcin PC, Miao B, Cook WD and Mitchell D (1994) Effects of size and curing on cylinder compressive strength of normal and high strength concretes. *ACI Materials Journal* **91(4)**: 349–354.

Aslani F and Nejadi S (2012a) Mechanical properties of conventional and self-compacting concrete: An analytical study. *Construction Building Materials* **36**: 330–347.

Aslani F and Nejadi S (2012b) Bond characteristics of steel fibre reinforced self-compacting concrete. *Canadian Journal of Civil Engineering* **39(7)**: 834–848.

Aslani F and Nejadi S (2012c) Bond behavior of reinforcement in conventional and self-compacting concrete. *Advances in Structural Engineering* **15(12)**: 2033–2051.

Aslani F and Nejadi S (2012d) Shrinkage behavior of self-compacting concrete. *Journal of Zhejiang University Science A* **13(6)**: 407–419.

Aslani F and Nejadi S (2012e) Bond characteristics of steel fiber and deformed reinforcing steel bar embedded in steel fiber reinforced self-compacting concrete (SFRSCC). *Central European Journal of Engineering* **2(3)**: 445–470.

ASTM (2000) *ASTM Standards 2000. Concrete and Aggregates*. ASTM International, West Conshohocken, PA, USA.

Bazant ZP (1984) Size effect in blunt fracture; concrete, rock, metal. *Journal of Engineering Mechanics ASCE* **110(4)**: 518–535.

Bazant ZP (1987) Fracture energy of heterogeneous material and similitude. *Proceedings of SEM-RILEM International Conference on Fracture of Concrete and Rock, Houston, TX, USA*, pp. 390–402.

Bazant ZP (1993) Size effect in tensile and compressive quasibrittle failures. *Proceedings of JCI International Workshop on Size Effect in Concrete Structures, Sendai, Japan*, pp. 141–160.

Bazant ZP and Xiang Y (1997) Size effect in compression fracture: splitting crack band propagation. *Journal of Engineering Mechanics ASCE* **123(2)**: 162–172.

Carrasquillo RL, Nilson AH and Slate FO (1981) Properties of high strength concrete subject to short-term loads. *ACI Materials Journal* **78(3)**: 171–178.

CEB-FIP (Comite Euro-International du Beton-Fédération Internationale de la Précontrainte) (1993) Model Code 1990. Bulletin D'Information No. 203/205. Comité Euro-International du Béton (CEB), Lausanne, Switzerland.

Chin MS, Mansur MA and Wee TH (1997) Effects of shape, size and casting direction of specimens on stress–strain curves of high strength concrete. *ACI Materials Journal* **94(3)**: 209–219.

Date CG and Schnormeier R (1981) Development and use of 48 inch concrete cylinders in Arizona. *Concrete International: Design and Construction* **3(7)**: 42–45.

Day RL and Haque MN (1993) Correlation between strength of small and standard concrete cylinders. *ACI Materials Journal* **90(5)**: 452–462.

EFNARC (2005) *The European Guidelines for Self-Compacting Concrete, Specification, Production and Use*. EFNARC, Farnham, UK.

Khayat KH and Roussel Y (1999) Testing and performance of fiber-reinforced, self-consolidating concrete. *Proceedings of Symposium on Self-Compacting Concrete, Stockholm, Sweden* (Skarendahl AP (ed.)), pp. 509–521.

Kim JK and Eo SH (1990) Size effect in concrete specimens with dissimilar initial cracks. *Magazine of Concrete Research* **42(153)**: 233–238.

Kim JK, Yi ST, Park CK and Eo SH (1999) Size effect on compressive strength of plain and spirally reinforced concrete cylinders. *ACI Structural Journal* **96(1)**: 88–94.

Kim JK, Yi ST and Yang EI (2000) Size effect on flexural compressive strength of concrete specimens. *ACI Structural Journal* **97(2)**: 291–296.

Kim JK, Yi ST and Kim JHJ (2001) Effect of specimen sizes on flexural compressive strength of concrete. *ACI Structural Journal* **98(3)**: 416–424.

Lessard M, Chaallal O and Aïtcin PC (1993) Testing high strength concrete compressive strength. *ACI Materials Journal* **90(4)**: 303–308.

Malhotra JM (1976) Are 48 inch concrete cylinders as good as 612 inch cylinders for quality control of concrete. *ACI Materials Journal* **73(14)**: 333–336.

Moreno J (1990) The state of the art of high-strength concrete in Chicago – 225W. Wacker Drive. *Concrete International: Design Construction* **12(1)**: 35–39.

Nasser KW and Kenyon JC (1984) Why not 36 inch cylinders for testing concrete compressive strength. *ACI Materials Journal* **81(1)**: 47–53.

Neville AM (1995) *Properties of Concrete*. Longman, UK.

Okamura H (1997) Self-compacting high-performance concrete. *Concrete International* **19(7)**: 50–54.

RTA (Regional Transportation Authority) (2006) *Materials Test Methods*, vol. 1. RTA, Chicago, IL, USA.

SA (Standards Australia) (1998) AS 3583. Methods of test for supplementary cementitious materials for use with portland cement. Standards Australia, Sydney, Australia.

SA (2000) AS 1478.1. Chemical admixtures for concrete, mortar and grout – admixtures for concrete. Standards Australia, Sydney, Australia.

SA (2001) AS 3582.2. Supplementary cementitious materials for use with portland and blended cement - Slag - Ground granulated iron blast-furnace. Standards Australia, Sydney, Australia.

SA (2006) AS 2350. Methods of testing portland and blended cements. Standards Australia.

SA (2010) AS 3972. General purpose and blended cements. Standards Australia, Sydney, Australia.

SA (2011) AS 1141. Methods for sampling and testing aggregates. Particle size distribution – sieving method. Standards Australia, Sydney, Australia.

Sleiman AI, Islam MS, Issa MA, Yousif AA and Issa MA (2000) Specimen and aggregate size effect on concrete compressive strength. *Cement and Concrete Aggregates* **22(2)**: 103–115.

Tokyay M and Özdemir S (1997) Specimen shape and size effect on the compressive strength of higher strength concrete. *Cement and Concrete Research* **27(8)**: 1281–1289.

Yi ST, Yang EI and Choi JC (2006) Effect of specimen sizes, specimen shapes, and placement directions on compressive strength of concrete. *Nuclear Engineering and Design* **236(2)**: 115–127.

WHAT DO YOU THINK?

To discuss this paper, please submit up to 500 words to the editor at www.editorialmanager.com/macr by 1 February 2014. Your contribution will be forwarded to the author(s) for a reply and, if considered appropriate by the editorial panel, will be published as a discussion in a future issue of the journal.